

Low temperature hydrogen generation from ammonia combined with lithium borohydride†‡

Liang Gao, Yan Hui Guo, Guang Lin Xia and Xue Bin Yu*

Received 13th August 2009, Accepted 18th September 2009

First published as an Advance Article on the web 29th September 2009

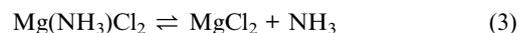
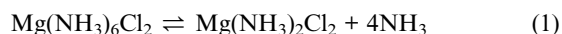
DOI: 10.1039/b916503g

A new complex material system, $\text{Mg}(\text{NH}_3)_n\text{Cl}_2\text{-nLiBH}_4$ (here n can be 1, 2 and 6), in which the MgCl_2 works as ammonia carrier but plays a crucial role in promoting the interaction between LiBH_4 and NH_3 to release hydrogen at temperature below 100°C , is reported.

Ammonia may be considered as a potential hydrogen carrier for hydrogen delivery and for off-board storage, such as at refueling stations and for stationary power applications. With the consideration of fast kinetic of ammonia absorption and desorption and feasibility of hydrogen release by catalytic cracking of ammonia, metal ammine complexes (e.g. $\text{Mg}(\text{NH}_3)_n\text{Cl}_2$, here n can be 1, 2 and 6) have been claimed as a new solid-state way of indirect hydrogen storage recently.¹⁻⁴ However, given the catalytic decomposition of ammonia from $\text{Mg}(\text{NH}_3)_n\text{Cl}_2$, there are still many significant challenges, including (a) high decomposition temperature of ammonia; (b) insufficient longevity and reliability of catalysts and other components; and (c) low hydrogen capacity in the system resulting from the accessional weight of MgCl_2 and catalysts *etc.*, which have to be overcome before it is available for on-board applications.¹

Herein, we report a new complex material system, $\text{Mg}(\text{NH}_3)_n\text{Cl}_2\text{-nLiBH}_4$ (here n can be 1, 2 and 6), in which the NH_3 molecules can react with BH_4 anion to generate H_2 without further combining with alkali to make NH_2 anion close to BH_4 anion on a molecular level, for example $\text{Li}_4\text{BH}_4(\text{NH}_2)_3$.⁵⁻⁷ In a series of experiments, we clearly demonstrated that $\text{Mg}(\text{NH}_3)_n\text{Cl}_2\text{-nLiBH}_4$ is efficient to release H_2 from both the ligands of NH_3 and the BH_4 anion at temperatures as low as 100°C . In addition, compared with the pure metal ammine complexes reported by Sørensen and co-workers, the hydrogen storage capacity is increased greatly in the $\text{Mg}(\text{NH}_3)_n\text{Cl}_2\text{-nLiBH}_4$ system due to the introduction of BH_4 anion.² It is deduced that protic (N–H) and hydridic (B–H) hydrogen atoms combine into H_2 , and MgCl_2 , working as a carrier of ammonia, fractionally takes part in the reaction.

A range of $\text{Mg}(\text{NH}_3)_n\text{Cl}_2$ (here n can be 1, 2 and 6) have been investigated as a solid form of hydrogen storage, and reversible ammonia adsorption and desorption can be described by eqn (1), (2) and (3).²⁻⁴



These stable ammine phases were mixed with LiBH_4 by ball milling for 6 min at mole ratios of 1:1, 1:2 and 1:6, respectively. Fig. 1 shows the TG-MS results for three mixtures, namely $\text{Mg}(\text{NH}_3)\text{Cl}_2\text{-LiBH}_4$ (sample I), $\text{Mg}(\text{NH}_3)_2\text{Cl}_2\text{-2LiBH}_4$ (sample II) and $\text{Mg}(\text{NH}_3)_6\text{Cl}_2\text{-6LiBH}_4$ (sample III). The onset dehydrogenation of sample III starts at around 75°C . Upon further heating, three major H_2 evolution peaks at 139°C , 216°C and 259°C with a shoulder at 292°C were observed, which is comparable with the three-step decomposition of $\text{Mg}(\text{NH}_3)_6\text{Cl}_2$ (see Fig. S1 in the ESI†). At higher temperature, one strong and broad H_2 peak appeared from 320°C to 517°C with a culmination at ca. 478°C , which results from the decomposition of excess LiBH_4 .⁸ For sample II, the onset dehydrogenation is about 72°C with two major H_2 peaks at 126°C (broad) and 246°C (Fig. 1(a)). In the case of sample I, only one apparent dehydrogenation peak at 240°C was observed. Furthermore, sample II and sample III exhibited vigorous emission of ammonia in the temperature range of $100\text{--}300^\circ\text{C}$, while sample I liberated only trace amounts of ammonia (Fig. 1(b)). The above results indicated that $\text{Mg}(\text{NH}_3)_n\text{Cl}_2$ combined with LiBH_4 results in a significant decrease of the hydrogen release from both NH_3 and LiBH_4 . In order to estimate the efficiency of NH_3 conversion, volumetric measurement of TPD for the three samples was conducted (see Fig. S2 in the ESI†). Based on the TG (Fig. 1(c)) and TPD results, the quantitative decomposition capacities of H_2 and NH_3 were calculated (see Table S1 in the ESI†). The calculation results indicated that sample I, sample II and sample III release 2.9, 5.1 and 10.5 equiv. of H_2 , accompanied by 0.08, 0.41 and 1.62 equiv. of NH_3 emission, respectively. The efficiency of NH_3 conversion for sample I, sample II and sample III is 91.6%, 78.9% and 72.4%, respectively. Clearly, $\text{Mg}(\text{NH}_3)\text{Cl}_2\text{-LiBH}_4$ showed the highest efficiency, which could be ascribed to its larger desorption enthalpy of ammonia than those of $\text{Mg}(\text{NH}_3)_2\text{Cl}_2$ and $\text{Mg}(\text{NH}_3)_6\text{Cl}_2$,² resulting in suppression of ammonia release until higher temperatures. Note that by designing a simple accessorial filter, we can restrain the emission of ammonia resulting in hydrogen generation with high purity (see Fig. S3 in the ESI†). This approach makes the $\text{Mg}(\text{NH}_3)_n\text{Cl}_2\text{-nLiBH}_4$ system exhibit prospective engineering applications for on-board hydrogen sources.

To understand the role of MgCl_2 in the hydrogen release of the $\text{Mg}(\text{NH}_3)_n\text{Cl}_2\text{-nLiBH}_4$ system, LiBH_4 was heated at 300°C for 3 h under pure ammonia atmosphere (about 1 bar). The result of ^{11}B NMR for the product shows scarcely detectable B atoms with chemical shifts comparable to the B atoms in LiBH_4 ⁹ (see Fig. S4 in

Department of Materials Science, Fudan University, Shanghai, China.
E-mail: yuxuebin@fudan.edu.cn

† L. Gao and Y. H. Guo contributed equally to this work.

‡ Electronic supplementary information (ESI) available: Detailed experimental procedures and measurement methods. Summary of NH_3 conversion ratio of the three samples. IR results of sample I. The TG and DTA result of $\text{Mg}(\text{NH}_3)_6\text{Cl}_2$. TPD results of hydrogen and ammonia release for three samples. The H_2 and NH_3 MS signals of $\text{NaBH}_4/\text{Mg}(\text{NH}_3)\text{Cl}_2$. See DOI: 10.1039/b916503g

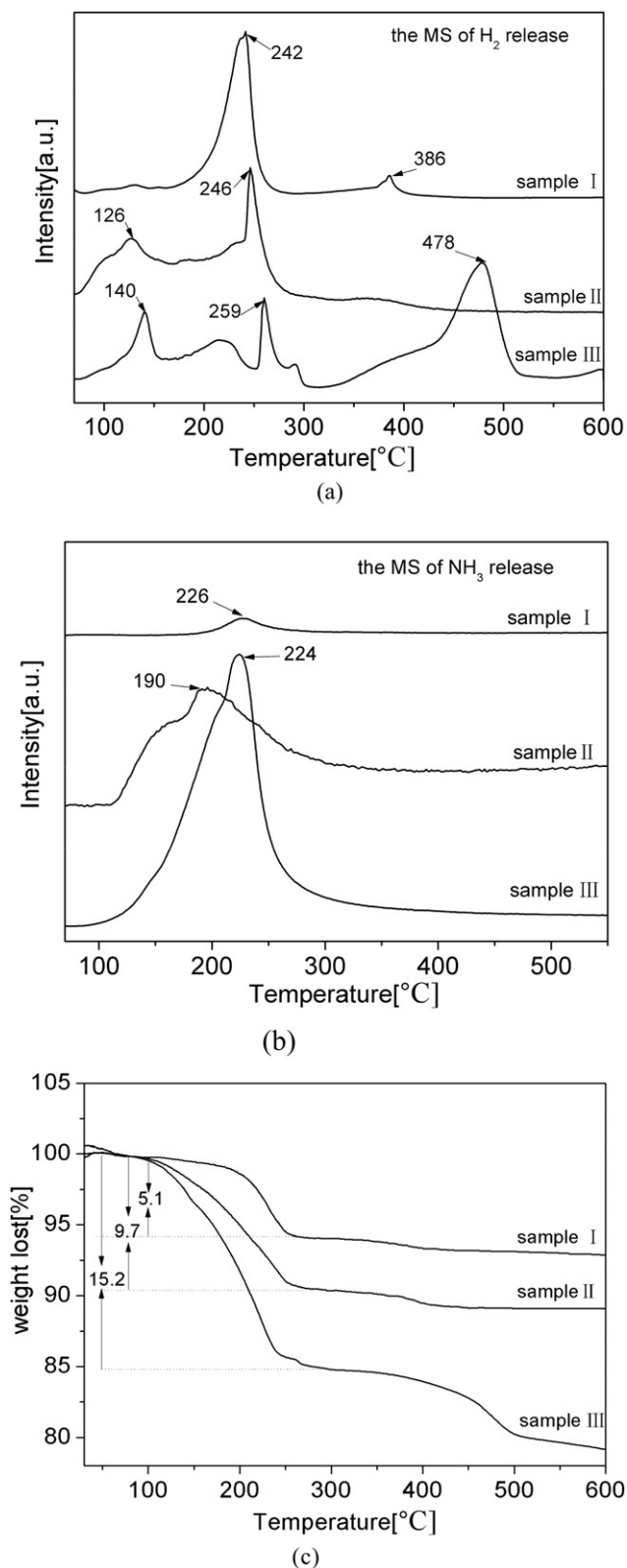


Fig. 1 a) Temperature dependence of H₂ release; b) temperature dependence of NH₃ release; c) TG results for samples I, II and III.

the ESI[†]), suggesting that pure NH₃ hardly reacts with LiBH₄ at 300 °C. It suggests that MgCl₂ plays a crucial role in promoting the hydrogen release in the Mg(NH₃)_nCl₂-nLiBH₄ system.

Fig. 2 shows the XRD patterns for sample I heated to different temperatures. The peaks in the as-prepared sample did not correspond to LiBH₄ or Mg(NH₃)Cl₂ (see Fig. S5 in the ESI[†]), suggesting that a new phase, the reflection of which should be assigned to a mixture of Mg(NH₃)Cl₂-LiBH₄, appeared. With the increase of the treatment temperature, the intensity of Mg(NH₃)Cl₂-LiBH₄ peaks decreased and transformed to MgCl₂ completely after 230 °C. It suggests that the hydrogen release is due to the reaction between ammonia and LiBH₄, and MgCl₂ only played the role of ammonia carrier. The improved dehydrogenation in Mg(NH₃)_nCl₂-nLiBH₄ may be due to the formation of Mg-N bonds, which lead to an increased positive charge of H^{δ+} in NH₃, thus promoting the combination of BH⁻·HN to produce H₂. Additionally, the onset dehydrogenation temperatures of sample II and sample III are about 100 °C lower than that of sample I. Although it is difficult to explain this clearly based on the current results, we are inclined to attribute this kind of discrepancy in temperature sensitivity to the different BH⁻·HN distances in sample I, sample II and sample III,¹⁰ which differ due to the different numbers of ammonia ligands of Mg(NH₃)_nCl₂ (n = 1, 2 and 6).

The fact that only MgCl₂ was detected in the XRD suggests that the final solid product for the reaction of ammonia and LiBH₄ is an amorphous structure. Combined with the TG results, the chemical composition of the amorphous structure is most likely to be (LiNBH). In order to confirm the possible routes for the hydrogen release and the possible chemical bond in the amorphous (LiNBH), the infrared spectra for sample I at RT, 50 °C, 150 °C, 200 °C and 250 °C were investigated (see Table S2 in the ESI[†]). The IR spectrum measured for sample I consists of several absorption bands in the NH bending, NH stretching, BH bending and BH stretching regions, and nearly the same positions of absorption peaks as for the substrates (Mg(NH₃)Cl₂ and LiBH₄) suggests that the ligand NH₃ and BH₄ anion remain intact within the structure.¹¹⁻¹³ There are no absorptions observed in positions expected for bridging B-H-B vibrations,

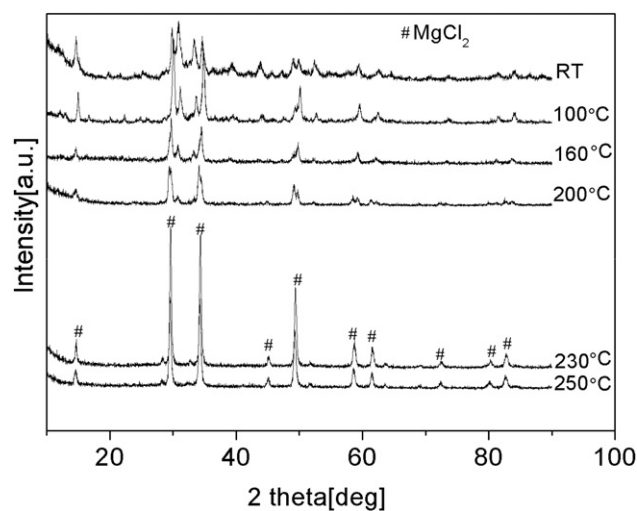


Fig. 2 XRD patterns of a) sample I, b) sample I after heating to 100 °C, c) 160 °C, d) 200 °C, e) 230 °C and f) 250 °C. The peaks of MgCl₂ are marked with #.

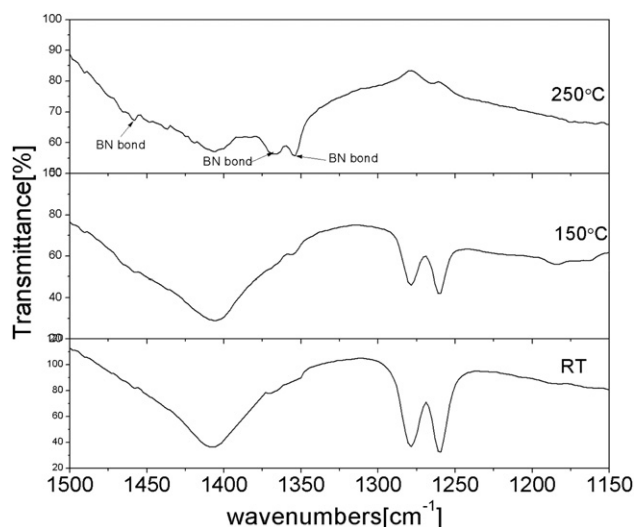


Fig. 3 FT-IR spectra (just cut from 1500cm^{-1} to 1100cm^{-1} to better expose the B–N region) of sample **I**: a) at room temperature; b) heated to $150\text{ }^{\circ}\text{C}$ and c) heated to $250\text{ }^{\circ}\text{C}$.

again consistent with the BH_4^- anion remaining intact.⁷ Consistent with the MS signal, there are no distinct differences between the IR spectra collected for sample **I** at RT and those after heat treatment at $50\text{ }^{\circ}\text{C}$ and $150\text{ }^{\circ}\text{C}$. After thermal decomposition at $250\text{ }^{\circ}\text{C}$, the bands in all of the NH stretching modes and two of the three NH bending modes are totally absent, but there are no distinct changes in BH bands because of no change in the BH stretching and bending regions. This is accompanied by the presence of three strong peaks (1457 cm^{-1} , 1366 cm^{-1} and 1354 cm^{-1}) as shown in Fig. 3, which are anticipated to be BN stretching modes and also agree with the strengthening of the B–N bond in AB (1382cm^{-1}) and NaNH_2BH_3 (1448 cm^{-1} and 1317 cm^{-1}).¹³ Disappearance of the bands assigned to NH stretching and bending modes is consistent with both disruption of the NH bonds due to evolution of H_2 and the observed emission of a small amount of ammonia. No changes in BH bands suggest that the amorphous product includes B–H bonds, confirming it has the structure of (LiBNH).

The ^{11}B NMR spectra for sample **I** at room temperature and after heat treatment at $200\text{ }^{\circ}\text{C}$, $250\text{ }^{\circ}\text{C}$ and $280\text{ }^{\circ}\text{C}$ are shown in Fig. 4. For the as-prepared sample, only a sharp line at -40.912 ppm is assigned to the boron nucleus in the tetrahedral BH_4^- units in LiBH_4 .^{9,14} After heat treatment at $200\text{ }^{\circ}\text{C}$, two new weak peaks are observed at -1.915 ppm and 18.064 ppm (Fig. 4). The appearance of those two weak peaks suggests that the chemical environment of fractional B atom shifts to lower field compared to the tetrahedral BH_4^- because of the formation of HBN_2 and BN_3 .¹⁵ In addition, a chemical shift, which is assigned to BH_4^- , is observed at -40.149 ppm . After desorption at $250\text{ }^{\circ}\text{C}$, one very weak peak at -18.655 ppm , which may be assigned to BNH_3 or BNH_2 , is observed along with the increase of the HBN_2 and BN_3 peaks (observed at 21.612 ppm and -1.647 ppm). Upon further heating at $280\text{ }^{\circ}\text{C}$ for 3h, the peaks corresponding to HBN_2 and BN_3 increased along with the peak of BH_4^- diminishing. However, the chemical shift, corresponding to BH_4^- , is always present (observed at -41.283 ppm), which is similar to the product of the decomposed LiAB and NaAB again (see Fig. S6 in the ESI†) Therefore, we surmise that the dehydrogenation

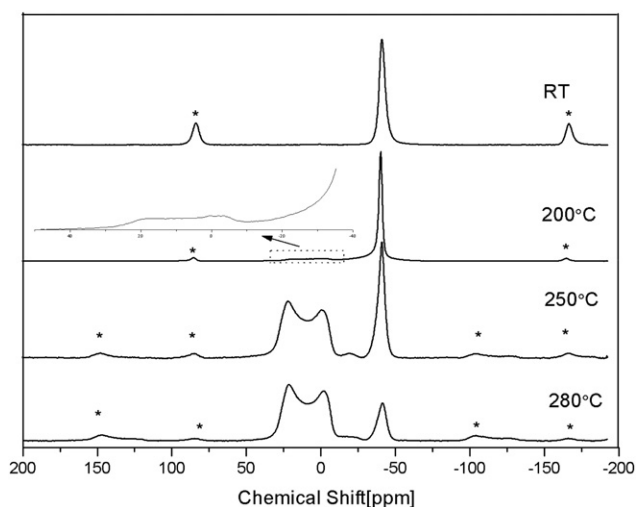


Fig. 4 The ^{11}B NMR of sample **I** recorded at 7.1T (96.3MHz): (a) at room temperature; (b) dehydrogenated after heat treatment at $200\text{ }^{\circ}\text{C}$; (c) dehydrogenated after heat treatment at $250\text{ }^{\circ}\text{C}$ for 15 min and (d) dehydrogenated after heat treatment at $280\text{ }^{\circ}\text{C}$ for 3h. Spinning side bands are marked with *.

mechanism of sample **I** is in some way the exact counterpart of LiAB or NaAB. Regardless of the detailed reaction pathway, according to the final products detected by XRD, FT-IR and ^{11}B NMR, and three molar equiv. of H_2 released (see Table S1 in the ESI†), we suggest that reaction (4) is responsible for the emission of H_2 mainly at $240\text{ }^{\circ}\text{C}$, which also shows the predominant reaction occurring during the thermal decomposition of sample **I**:



Eqn (4) explains the presence of the MgCl_2 phase detected by XRD, and also support the presence of three IR peaks (1457 cm^{-1} , 1366 cm^{-1} and 1354 cm^{-1}), as shown in Fig. 2, which are anticipated to be BN stretching modes. The observed HBN_2 and BN_3 in ^{11}B NMR spectra are consistent with the B atom environment in a borazine-like or poly-borazine-like compound: (LiBNH), which was reported by Xiong *et al.* recently.¹⁶ However, reaction (4) does not explain the B site of BH_4^- observed in ^{11}B NMR spectra (note that nearly the same B site can be found in the decomposition of our home made lithium amidoborane). We suggest that the presence of BH_4^- is correlated with the emission of fractional NH_3 from sample **I** which results in the surplus of BH_4^- anion. MS signals of pure $\text{Mg}(\text{NH}_3)\text{Cl}_2$ show a weak peak corresponding to NH_3 release at around $227\text{ }^{\circ}\text{C}$ (see Fig. S7 in the ESI†), consistent with the main emission of NH_3 in sample **I** detected at around $227\text{ }^{\circ}\text{C}$ (Fig. 1b). The thermodynamic similarity in NH_3 release reveals that the mechanism of ammonia emission in sample **I** is nearly the same as that for pure $\text{Mg}(\text{NH}_3)\text{Cl}_2$. Furthermore, the calculated weight loss of reaction (4) is about 4.5%, which is about 0.7% lower than the TG result (note that NH_3 is much heavier than H_2), which also can be explained by the emission of a small amount of ammonia in sample **I**. The emission of NH_3 of sample **I** is likely due to incomplete contact of the particles in the solid state or fractional $\text{Mg}(\text{NH}_3)_x\text{Cl}_2$ (here $x > 1$) which may contaminate our home made $\text{Mg}(\text{NH}_3)\text{Cl}_2$, and the ligand NH_3 fails to take part in chemical reaction (4) with stoichiometric LiBH_4 .

It is worth noting that a similar performance can be achieved by mixing $\text{Mg}(\text{NH}_3)\text{Cl}_2$ with other borohydrides, such as NaBH_4 , $\text{Mg}(\text{BH}_4)_2$ and $\text{Ca}(\text{BH}_4)_2$. As an example, the result of NaBH_4 - $\text{Mg}(\text{NH}_3)\text{Cl}_2$ was examined (see Fig.S8 in the ESI†). The MS signal of NaBH_4 - $\text{Mg}(\text{NH}_3)\text{Cl}_2$ showed one major H_2 peak at around 235 °C, which is consistent with the dehydrogenation temperature of LiBH_4 - $\text{Mg}(\text{NH}_3)\text{Cl}_2$. It can be expected that $\text{M}^{n+}(\text{BH}_4)^{-n}$ (regardless of which kind of metal cation the M stands for), borohydrides are always effective species in suppressing the emission of ammonia from $\text{Mg}(\text{NH}_3)_n\text{Cl}_2$.

In summary, we have demonstrated a new multicomponent hydrogen storage system of $\text{Mg}(\text{NH}_3)_n\text{Cl}_2$ - $n\text{LiBH}_4$, in which MgCl_2 plays the role of ammonia carrier and the hydrogen in the ligand NH_3 is released by combining with BH_4^- anion at temperatures below 100 °C. These results indicated that, compared with catalytic cracking of ammonia, keeping ammonia in the form of $\text{Mg}(\text{NH}_3)_n\text{Cl}_2$ and releasing the hydrogen from the ligand NH_3 through reacting with additives at lower temperatures may be one more efficient approach towards an ammonia-mediated hydrogen economy.

Notes and references

- G. Thomas and G. Parks, *Potential Roles of Ammonia in a Hydrogen Economy*, http://hydrogen.energy.gov/pdfs/nh3_paper.pdf, 2006.
- R. Z. Sørensen, J. S. Hummelshøj, A. Klerke, J. B. Reves, T. Vegge, J. K. Nørskov and C. H. Christensen, *J. Am. Chem. Soc.*, 2008, **130**, 8660.
- C. H. Christensen, R. Z. Sørensen, T. Johannessen, U. J. Quaade, K. Honkala, T. D. Elmøe, R. Køhlera and J. K. Nørskov, *J. Mater. Chem.*, 2005, **15**, 4106.
- J. S. Hummelshøj, R. Z. Sørensen, M. Yu. Kustova, T. Johannessen, J. K. Nørskov and C. H. Christensen, *J. Am. Chem. Soc.*, 2006, **128**, 16.
- Y. Nakamori, A. Niritake, G. Kitahara, M. Aoki, T. Noritake, K. Miwa, Y. Kojima and S. Orimo, *J. Power Sources*, 2006, **155**, 447.
- F. E. Pinkerton, G. P. Meisner, M. S. Meyer, M. P. Balogh and M. D. Kundrat, *J. Phys. Chem. B*, 2005, **109**, 6.
- P. A. Chater, W. I. F. Dvaid, S. R. Johnson, P. P. Edwards and P. A. Anderson, *Chem. Commun.*, 2006, 2439.
- A. Zuttel, P. Wenger, S. Rentsch, P. Sudan, P. Mauron and C. Emmenegger, *J. Power Sources*, 2003, **118**, 1.
- S. J. Hwang, R. C. Bowman, J. W. Reiter, J. Rijssenbeek, G. L. Soloveichik, J. C. Zhao, H. Kabbour and C. C. Ahn, *J. Phys. Chem. C*, 2008, **112**, 3164.
- H. Wu, W. Zhou and T. Yildirim, *J. Am. Chem. Soc.*, 2008, **130**, 14834.
- T. J. Marks and J. R. Klob, *Chem. Rev.*, 1977, **77**, 263.
- R. Plus, *J. Raman Spectrosc.*, 1973, **1**, 551.
- K. J. Fijalkowski and W. Grochala, *J. Mater. Chem.*, 2009, **19**, 2043.
- L. Mosegaard, B. Møller, J. Jørgensen, U. Bösenberg, M. Dornheim, J. C. Hanson, Y. Cerenius, G. Walker, H. J. Jakobsen, F. Besenbacher and T. R. Jensen, *J. Alloys Compd.*, 2007, **446–447**, 301.
- C. Gervais, J. Maquet, F. Babonneau, C. Duriez, E. Framery, M. Vaultier, P. Florian and D. Massiot, *Chem. Mater.*, 2001, **13**, 1700.
- Z. T. Xiong, C. K. Yong, G. Wu, P. Chen, W. Shaw, A. Karkamkar, T. Autrey, M. O. Jones, S. R. Johnson, P. P. Edwards and W. I. F. David, *Nat. Mater.*, 2008, **7**, 138.